

EVALUATION OF MEAN WAVE OVERTOPPING AND MAXIMUM INDIVIDUAL WAVE OVERTOPPING ON ROCK REVETMENT

Mohd Shahrizal Ab Razak*, Amirah Afiqah Masri, Noor Asiah Mohamad, Nor Syamimi Rosdi, Abdul Rehman Khan

Department of Civil Engineering, Faculty of Engineering
Universiti Putra Malaysia, Malaysia

Article history

Received

6 May 2024

Received in revised form

4 July 2024

Accepted

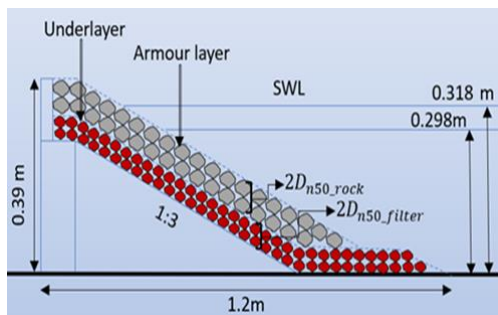
10 July 2024

Published Online

20 February 2025

*Corresponding author
ar_shahrizal@upm.edu.my

Graphical abstract



Abstract

An accurate estimation of wave overtopping discharge on rock revetment is important to protect coastal areas from possible hazards. The mean discharge value is often used in the coastal structural design. However, the anticipated impact of the maximum volume of overtopping by individual waves is expected to be significant in wave overtopping analysis. This research investigates the mean discharge of wave overtopping and maximum volume of overtopping by individual wave using two-dimensional (2D) physical model tests. The rock revetment model consists of armour layer with $D_{50}=46$ mm, a filter layer with $D_{50}=13$ mm, and an impermeable core, with a thickness of $2D_{50}$ for armour and filter layers. Wave overtopping volumes obtained from physical tests were then compared to EurOtop empirical formulae. The results showed that the variability of wave overtopping increases when the wave height and water level increase. This variation falls within the specified interval boundaries by EurOtop empirical methods, with the exception of the lower maximum volume of overtopping by individual waves. Furthermore, the findings indicate that the maximum volume of overtopping by individual waves can exceed the mean wave overtopping volume by up to 85%.

Keywords: Mean wave overtopping discharge, maximum individual wave overtopping volume, physical model tests, rock revetment

Abstrak

Anggaran yang tepat bagi kadar alir limpahan ombak pada struktur lapis lindung batu adalah penting untuk melindungi kawasan pantai daripada bahaya yang mungkin berlaku. Nilai purata kadar alir sering digunakan dalam reka bentuk struktur pantai. Walau bagaimanapun, isipadu maksima limpahan ombak individu dijangka mempunyai kesan yang lebih besar terhadap struktur. Oleh itu, kajian ini menyiasat kadar alir purata limpahan ombak dan isipadu maksimum limpahan ombak individu melalui ujian permodelan fizikal dua dimensi (2D) di Makmal Hidraulik Universiti Putra Malaysia. Model lapis lindung batu tersebut terdiri daripada lapisan pelindung utama dengan $D_{50}=46$ mm, lapisan penyaring dengan $D_{50}=13$ mm, dan lapisan teras tidak telap, dengan ketebalan $2D_{50}$ untuk lapisan pelindung utama dan lapisan penyaring. Isipadu limpahan ombak yang diperoleh daripada ujian permodelan fizikal kemudiannya dibandingkan dengan formula empirikal Eurotop. Keputusan menunjukkan bahawa variasi limpahan ombak meningkat apabila ketinggian ombak dan paras air meningkat. Variasi ini termasuk dalam sempadan selang yang ditentukan oleh kaedah empirikal EurOtop kecuali untuk isipadu maksima limpahan

ombak individu yang lebih rendah. Keputusan juga menunjukkan bahawa isipadu maksima limpahan ombak individu adalah sehingga 85% lebih besar daripada isipadu purata limpahan ombak.

Kata kunci: Purata limpahan ombak, isipadu maksimum limpahan ombak individu, Ujian pemodelan fizikal, lapis lindung batu

© 2025 Penerbit UTM Press. All rights reserved

1.0 INTRODUCTION

Understanding wave overtopping phenomena is pivotal for effective coastal management, particularly in the design and maintenance of sea dikes aimed at flood protection [1]. With climate change influencing water depths and wave heights, the dynamics of overtopping become more complex and challenging to predict accurately. Therefore, the development of precise assessment tools is crucial for managing these complexities across diverse coastal environments. Beyond simply measuring total overtopping volume, individual wave events play a critical role in assessing the risk posed to coastal defenses [2]. By analyzing the probability distribution of these events, factors such as maximum flow velocity and layer thickness can be evaluated, directly impacting the safety and stability of sea dikes [2].

The predominance of irregular waves further complicates the design process, necessitating careful consideration of their turbulent and complex nature [3]. By integrating statistical estimations with detailed analyses of wave characteristics, engineers gain valuable insights crucial for the effective design of sea dikes. Advancements in measurement and modeling technologies are thus essential for developing robust sea defense systems that safeguard coastal communities and critical infrastructure.

In the initial studies of wave overtopping, the measurement of wave overtopping focused on the average rate of overtopping. Saville and Caldwell [4] conducted the initial simulations of wave overtopping back in 1953. This initial model revealed that, when the value of seawall height measured from sea level i.e. freeboard over wave height (R_c/H_{m0}) falls between 0 and 0.4, the value of overtopping will be at its largest. They also found that wave steepness, ϵ a ratio between wave height and wavelength, (H_0/L_0) was a crucial factor [5]. In recent years, the wave overtopping formulas of Van der Meer [6],[7] have been adopted in various guidelines for the development of coastal structure.

A recent paper by Khosseh [2] has provided a revised analysis of overtopping parameters related to individual wave overtopping. The study concluded that the maximum discharge from individual wave overtopping during an overtopping event could be a thousand times greater than the average

overtopping discharge. This substantial increase in maximum individual wave overtopping has the potential to intensify erosion at the base of coastal structures and could lead to structural failure.

In the past, overtopping has caused several dike collapses, dike breaches, and significant flooding. According to China's National Marine Hazard Mitigation Service, a major mechanism of sea-dike failure occurs during wave overtopping, resulting in a certain amount of damage, breached, or destroyed structures along the 70 % of China's coastline that is protected by coastal structures [8]. In 1889, a South Dark earth fill dam in the United States failed owing to overtopping, which lasted for three and a half hours and resulted in the loss of 2,200 lives [9]. The failure was prevalent owing to erosion process during the extreme overtopping event. On the other hand, according to research that was conducted in the Germany and Netherlands, dike breaching was mostly caused by overtopping, resulting in erosion along the interior side of the slope or, more commonly, slide failure, or possibly both [10]. In instances where these failures occurred, the design structures ignored the wave overtopping criterion on the assumption that no overtopping would occur [10]. However, a well-designed slope structure need to consider the unpredictability of sea level rise and the escalating frequency and severity of coastal flooding globally, thus preventing extreme overtopping events.

Previous research on wave overtopping primarily focused on mean discharge per meter (q) as the key parameter for traditional coastal structures. However, this approach fails to consider the most critical factor: the potential for individual wave overtopping volumes to be thousands of times greater than the average. These large, infrequent events pose the most severe risk of damage [11], particularly for rock revetments. Unlike traditional structures, rock revetments are vulnerable to the immense forces exerted by individual waves; forces not adequately captured by solely considering mean overtopping. Laboratory and field studies have demonstrated that the maximum individual wave overtopping discharge significantly exceeds the mean overtopping discharge [2]. Therefore, determining individual wave overtopping has become crucial to avoid these hazardous events that threaten coastal structures and people. This study addresses this gap in knowledge by employing a physical modeling setup to quantify both mean and

maximum individual wave overtopping. By comparing these results with established empirical equations, the findings can guide engineers in selecting the most appropriate wave overtopping estimation method for future designs.

1.1 Wave Overtopping

When the crest of a coastal structure is surpassed by the predicted wave height, it leads to wave overtopping, causing water to overflow [12]. During this phenomenon, the wave is partially reflected to the sea and partially passed over the structure, and the wave overtopping refers to the portion of the wave that overflows the structures. Two simple direct responses are used to determine wave overtopping which are mean wave overtopping discharge and individual wave overtopping volume. These metrics are frequently utilized in designing a safe and sustainable coastal structure with tolerable wave overtopping discharge. In addition, more complex or non-direct responses can also be observed to evaluate the impact of wave overtopping, such as the velocities of the overflowing waves, the flow thickness, post-overtopping impulsive and non-impulsive pressures of the waves. Furthermore, several important variables should be considered as they will affect the rate of wave overtopping. Those variables include wave height, wave period, wave steepness, roughness coefficient of the coastal structure and crest freeboard. Majority of these factors are typically applied to design coastal structures as an effort to enhance the current construction design.

The inaugural European manual on wave runup and wave overtopping for coastal structures, known as EurOtop, was published in 2007 [13]. The developed equations in EurOtop [14] were built based on experimental data from Crest Level Evaluation of Coastal Structures (CLASH) research with the intention of developing a general prediction technique for a crest height design and estimation [15]. The EurOtop manual [13] presents two formulas; breaker, and non-breaker wave conditions, that are generated based on the surf similarity number. When overtopping reaches its peak for non-breaker conditions, it becomes independent of wave steepness, which means it does not define a range of validity for the formulas [16]. Consequently, it leads to inaccurate results beyond the validated area.

Recently, an updated version of the EurOtop manual has improved their prediction accuracy based on additional experimental datasets from over 12,000 wave overtopping experiments on all types of coastal structures [17]. A recent study by Koosheh [2], used this new database with an additional 140 tests on rock revetment to further investigate the accuracy and limitation of existing empirical equations of average overtopping discharge specifically on rock revetment structure. In the research, the effect of different slope conditions was ignored, and more attention was given to the effect of different crest freeboard heights and wave steepness. The study

concluded that lower wave steepness contributes to larger wave overtopping events.

Bruce [18] evaluated the impact of mean wave overtopping discharge on several types of armour layer, resulting in a database of varying values for the roughness coefficient, γ_f . This roughness coefficient, γ_f is applicable to breakwater structures with a slope of 1:1.5. They also found that in rock case, the value of the roughness coefficient decreases as the angle of the slope decreases. Hence, only structures with slope 1:1.5 are fitted to follow the roughness coefficient value.

Strain *et al.*, [19] compared how effective mangroves and rock revetments are for coastal protection in Victoria, Australia. It shows that both mangroves and rock revetments reduce wave strength in sheltered areas, but rock revetments generally achieve greater wave reduction per meter in certain locations. Despite being more expensive initially, rock revetments occupy less land compared to mangroves. Furthermore, the rock materials employed in revetments exhibit long-lasting durability with minimal reported failures [20]. Nevertheless, several countries, including the Netherlands, Singapore, and Kuwait, face challenges due to the unavailability of a sufficient quantity of rocks with suitable properties, which complicates the implementation of rock revetments in these regions[21].

The amount of water overtopped during an overtopping event varies significantly from the mean wave overtopping rate due to the random nature of waves. To construct a safe coastal defence structure, it is thus impossible to depend merely on the mean overtopping discharge. Hence, due to the irregular character of waves, the individual wave overtopping volume is an important measure for predicting probable overtopping dangers under certain wave circumstances.

1.2 Empirical Formula of Wave Overtopping

Mean wave overtopping discharge: As a result of the irregular and dynamic characteristics of wave overtopping, a precise deterministic analysis of this phenomena is challenging [14]. Using empirical formulas drawn from experimental data is the most straightforward method for calculating the overtopping rate. EurOtop 2008 [13] has been updated to EurOtop 2018 [14], which improves the equation for low freeboard area and zero freeboard conditions. This study employs the most recent equation of mean wave overtopping, which is defined as

$$\frac{q}{\sqrt{g \cdot H_{m0}^3}} = 0.09 \cdot \exp \left[- \left(1.5 \frac{R_c}{H_{m0} \cdot \gamma_f \cdot \gamma_\beta \cdot \gamma_v} \right)^{1.3} \right] \quad (1)$$

where q represents the mean wave overtopping discharge, g denotes gravity acceleration, R_c indicates crest freeboard, H_{m0} signifies incident wave

height, γ_f and γ_r represents the roughness factor. In this study, no oblique wave attack and wall above the structure is present. Therefore, γ_β and γ_v are assumed to be 1.0.

Roughness factor, γ_f can be determined from the previous study done by Bruce [18]. However, it is only applicable for a structure slope of 1:1.5. Therefore a modification needs to be done to increase the accuracy of the output. Christensen [22] applied the modified roughness factor by

$$\gamma_{f\text{surging}} = \gamma_f + \frac{(\epsilon_{m-1,0} - 1.8)(1 - \gamma_f)}{8.2} \quad (2)$$

The roughness factor must be dependent on wave steepness, $\epsilon_{m-1,0}$ because the longer the wave, the larger the volume of water that will fill the voids between the rock layer and cause majority of the water to flow in the outermost layer of the breakwater [22]. They discovered that long-wave results are more reliable when using the modification roughness factor.

Maximum individual wave overtopping volume: The estimation of the maximum individual wave overtopping, V_{max} at the rock revetment structure can be determined through the number of overtopping waves, N_{ow} .

$$V_{max} = a \cdot [\ln(N_{ow})]^{\frac{1}{b}} \quad (3)$$

where a is the scale parameter and b is the shape parameter. To estimate the scale parameter, a Van der Meer [14] proposed an empirical formula as shown in Equation 4. This equation displays that the scale parameter a is contingent upon the shape parameter b , mean wave overtopping discharge q , average wave period T_m and probability of overtopping event P_{ov} which can be determined using Equation 5.

$$a = \left(\frac{1}{r(1 + \frac{1}{b})} \right) \left(\frac{q \cdot T_m}{P_{ov}} \right) \quad (4)$$

$$P_{ov} = \frac{N_{ow}}{N_w} = \exp \left[- \left(\frac{R_c \cdot D_n}{0.19 H_{m0}^2} \right)^{1.4} \right] \quad (5)$$

R_c indicates freeboard level and D_n indicates a nominal diameter of armour unit. This equation illustrates that both the dimensions of the armor unit and the height of the waves play a role in affecting the likelihood of wave overtopping.

According to Zanuttigh [23], the shape parameter value, b of 0.75 is recommended for sloped structures. On the other hand, Christensen [22] revealed that the shape parameter, b for rubble mound structures may be somewhat varied as shown in Figure 1. Empirical formulae for the shape parameter, b was derived from Figure 1 and shown in Equation 6. For a rubble mound structure, the shape parameter has a minimum value of 0.85, relatively bigger compared to a smooth slope structure.

$$b = 0.85 + 1500 \left(\frac{q}{g H_{m0} T_{m-1,0}} \right)^{1.3} \quad (6)$$

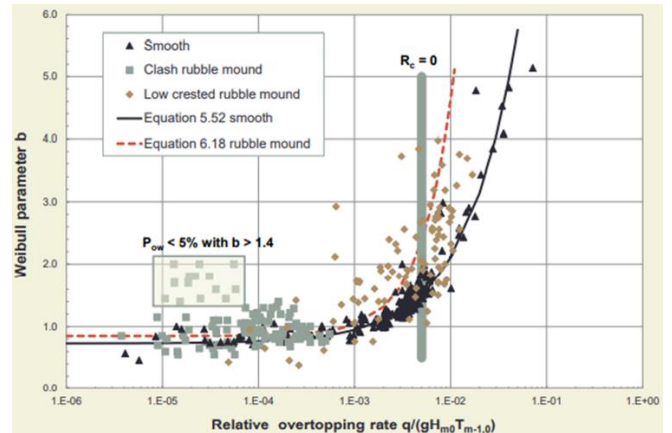


Figure 1 A relationship between relative overtopping rate and the Weibull parameter, b for smooth slope structures and rubble mound slope structures [14]

2.0 METHODOLOGY

2.1 Experimental Facility

A series of wave overtopping experiments were conducted at the Hydraulic Laboratory of the Civil Engineering Department, Faculty of Engineering, Universiti Putra Malaysia. These experiments took place in a wave flume, as shown in Figure 2, specifically designed for such investigations on rock revetments.

The wave flume is 1.5 m width, 20 m long (17m effective length), and 1.2 m high, as shown in the schematic diagram of Figure 3. In this study, irregular wave conditions were generated using the piston-type wave paddle, which is capable of producing both regular and irregular waves. The irregular waves were specifically generated based on the JONSWAP wave spectrum.

Near the rock structure, four wave gauges were positioned to capture the incident waves, while an extra wave gauge was positioned close to the wave paddle to monitor the number of waves generated during each test. The wave reflection analysis was determined using the least squares method, based on four wave probes, located in front of the structure with known distances between them and all fixed at a consistent level as shown in Figure 4. A weight scale was placed below the overtopping tank to record the mass of each overtopping event as shown in Figure 5. The overtopping water was channelled through a sloping chute into the overtopping tank.

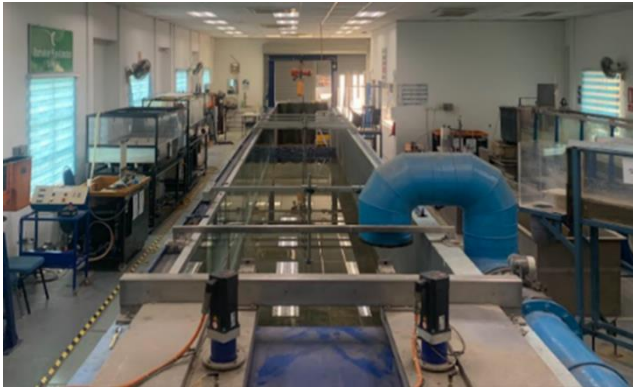


Figure 2 Wave flume in Hydraulic laboratory of Civil Engineering Department, Universiti Putra Malaysia

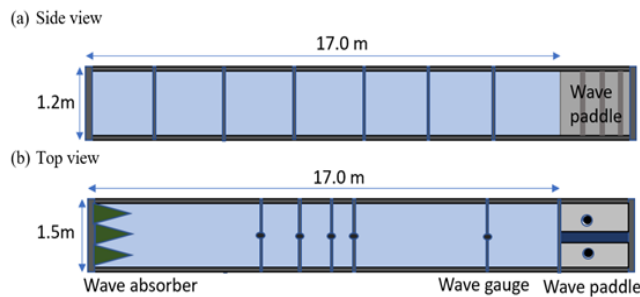


Figure 3 Schematic diagram of the wave flume from (a) side view and (b) top view with main dimensions

Two digital cameras were used; one was positioned at the right side of the model to capture the incidence of overtopping waves, and another was installed at the rear side of the overtopping tank to record the mass of every overtopping wave in each test as shown in Figure 6. To convey the overtopping water into the tank, a chute with dimensions of 0.105 m width and 1.22 m length was fixed at the crest of the rock revetment wall, and the chute's end was placed on the overtopping tank with a slope of 6%.

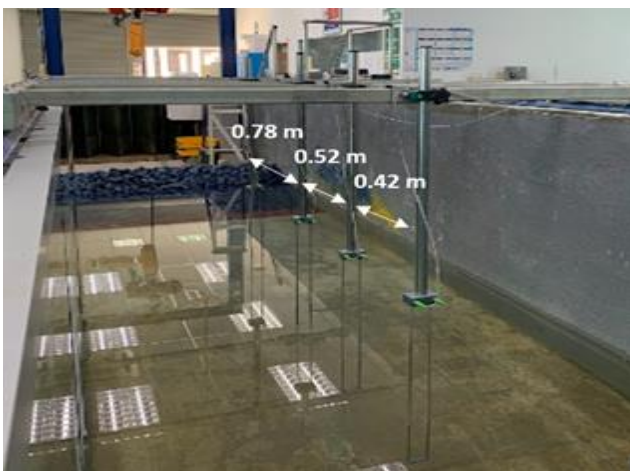


Figure 4 Wave probes positioning at a specified distance inside the wave flume



Figure 5 Overtopping chute and overtopping tank placed on weighting scale to collect overtopping waves and measure overtopping volume

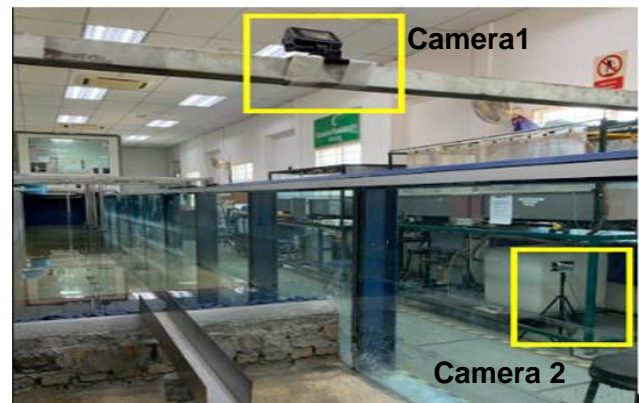


Figure 6 Two digital cameras installed at different positions to record the number of overtopping wave and water mass of every overtopping wave

2.2 Structural Configuration

The wave overtopping tests were conducted on rock revetment structure with a structural height of 0.39 m and side slope of 1:3, as shown in Figure 7.

The rock revetment structure as shown in Figure 8 contains an impermeable core of compacted sand with a thin mortar layer on the top, an underlayer with $D_{n50} = 13$ mm and an armour layer with $D_{n50} = 46$ mm. A minimum thickness of $2D_{n50}$ was considered for both armour layer and underlayer. The roughness factor of the structure was determined using Equation 2, as proposed by [22].

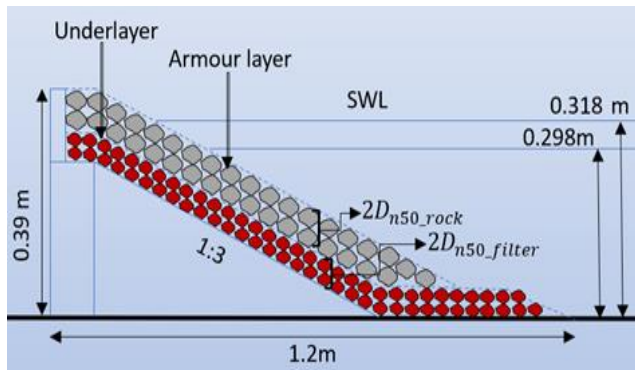


Figure 7 Test configuration of rock revetment, with structure height of 0.39 m, seaward slope of 1:3 and minimum thickness of $2D_{50}$ for both armour layer and filter layer. Two varying water depths were examined i.e 0.298 m and 0.318 m

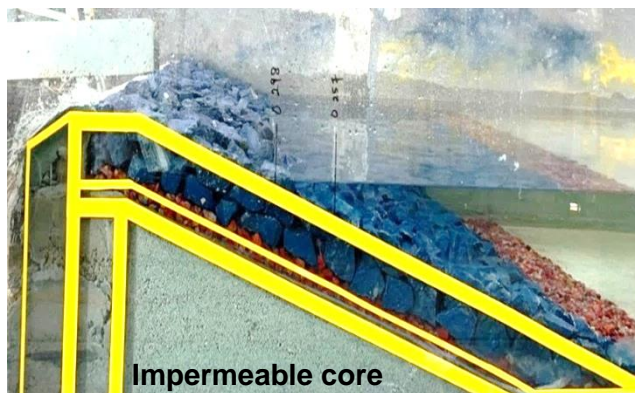


Figure 8 A constructed rock revetment model in the wave flume. The blue coloured rocks and red coloured rocks represent armour layer and underlayer, respectively

2.3 Experimental Procedure

The experimental procedure of wave overtopping measurement on rock revetment begins with an experimental setup, continued with the laboratory experiment and data processing, and concluded with data analysis. Each stage is presented as follows:

(a) Experimental setup

After the rock revetment model was constructed in the wave flume, water was added into the flume according to the first experimental water depth. The weighting scale was reset to zero after placing the overtopping tank on the weighting platform, to ensure that the recorded mass is merely the weight of overtopping water. Five wave probes were then placed securely in the required positions to allow the calibration process to begin. The calibration process was repeated for every different water level test to ensure the accuracy of the results. The calibration of the wave gauges is achieved when the R^2 value exceeds 0.99.

(b) Laboratory experiment

Based on the parameters provided in the HR Merlin software, irregular waves were generated. Input

parameters such as significant wave height (H_s), peak wave period (T_p), water depth (d), spectral parameter such as Jonswap spectrum with peak enhancement factor (γ) of 3.3 and a random seed number were inputted into the HR Merlin software. Wave seed number is a random number where every seed number will result in a different value and frequency of maximum wave rise and maximum wave fall. As individual wave overtopping volume was observed for this experiment, a wave seed number that generates peak waves with large period distance is used to prevent a continuous wave overtopping occurrence. In this study, two water depths were tested i.e $h = 0.298$ m and 0.318 m, leading to two different freeboards i.e $R_c = 0.093$ m and 0.073 m, respectively. The freeboards were selected based on the expected overtopping discharge. First, the mean overtopping discharge should be more than 1×10^{-6} m³/s/m because discharge below that value is considered zero overtopping. Second, the total overtopping volume should not be large enough to exceed the overtopping tank capacity, which complicates the individual overtopping measurement. Each freeboard was tested with three different wave heights, H_s which were 0.08 m, 0.09 m and 0.10 m. Test scenarios are shown in Table 1. Each test program was repeated three times to check the consistency of the result. In this study, a total of 18 experimental tests were performed.

Table 1 Experimental program for overtopping measurement on rock revetment

Freeboard, R_c (m)	Water depth, h (m)	Wave Height, H_s (m)	Wave Period, T_p (s)	Reflection Coefficient C_r (-)
0.093	0.298	0.08	1.60	0.223
		0.09	1.70	0.224
		0.10	1.79	0.228
0.073	0.318	0.08	1.60	0.236
		0.09	1.70	0.238
		0.10	1.79	0.239

Each test was performed for 20 minutes to achieve approximately 1,000 number of irregular waves. The signal from the wave probes were transmitted into HR DAQ software and thus the output data were obtained after the test ended. The output data include the spectral waves such as H_{m0} , T_{m-0} , and N_w . The video camera was turned on as soon as the wave paddle begins to generate wave to record the overtopping events over the test duration.

(c) Data processing

Data processing begins with the analysis of wave reflection. The reflection analysis was discussed in Section 2.1 by using the least square method and the coefficients extracted from the HR DAQ software are shown in Table 1. In all tests, it is inferred that about 22 to 24% of incident waves were reflected from the structure. To check the data consistency between

measured data and predicted data, the results comparison between the measurement and predictive equations was evaluated. The measured mean wave overtopping discharge (q_{meas}) was compared against the predicted overtopping (q_{pred}). $q_{predict}$ is determined based on Equation 1, while q_{meas} is determined by averaging the volume of water collected in the overtopping tank over the test duration. Likewise, the measured maximum individual wave overtopping volume is compared with the predicted maximum overtopping volume ($V_{max,pred}$). $V_{max,pred}$ is determined using Equation 3, while the $V_{max,meas}$ is determined based on the maximum volume of water collected for every overtopping event.

(d) Data analysis

The final stage is the discussion of the results and findings. The results were presented in terms of relationships between different parameters such as (i) mean overtopping discharge against wave height and water depth, (ii) maximum individual overtopping discharge against wave height and water depth, (iii) comparison between measured and predicted mean and maximum individual wave overtopping and (iv) comparison between mean wave overtopping volume and maximum individual wave overtopping volume.

2.4 Methods of Analysis

Wave outputs were obtained from the HR DAQ software. The number of waves, N_w were extracted from the zero-crossing statistics analysis which were then computed using Equation 5 to measure the probability of wave overtopping event, P_{ov} . The zero-moment wave period, T_{m-0} and the spectral wave height, H_{m0} were extracted from the spectral density analysis. As the reflected waves may interfere with incident waves, a reflection analysis was performed to eliminate the reflected waves. The incident wave height, H_i was obtained using Equation 7,

$$H_i^2 = \frac{H_{m0}^2}{(1 + C_r^2)} \quad (7)$$

where the spectral wave height, H_{m0} was obtained from the HR DAQ data processing output and reflection coefficient, C_r was obtained from the reflection analysis result, as shown in Table 1. The incident wave height, H_i was used to calculate the predicted mean wave overtopping discharge, q and maximum individual wave overtopping volume, V_{max} .

To compare the variation in mean wave overtopping volume and maximum individual wave overtopping volume, a percentage difference was used, similar to the equation used in [24], as expressed in Equation 8,

$$Diff \% = \left(1 - \frac{X_{min}}{X_{max}}\right) \times 100 \quad (8)$$

where X_{min} is the minimum value and X_{max} is the maximum value. In this study, the minimum value represents the mean wave overtopping volume and the maximum value is the maximum individual wave overtopping.

Three main statistical error indices were used to evaluate the performance of predictive equations as compared to measurement. The root mean square error (RMSE) measures the difference between the values predicted by a predictive equation and the measurements. The mean absolute percentage error (MAPE) quantifies the magnitude of error in percentage terms, offering insight into the predictive performance of an empirical model. The Nash-Sutcliffe efficiency (NSE) compares the residual variance of the empirical model to the variance of the measured data. A perfect model fit to the observed data yields an NSE of 1, indicating a complete match between predicted and observed values. The RMSE, MAPE and NSE are expressed in Equation 9, 10, and 11, respectively.

$$RMSE = \sqrt{\frac{\sum_{i=1}^n (Measr_i - Model_i)^2}{n}} \quad (9)$$

$$MAPE = \left[\frac{1}{n} \times \sum_{i=1}^n \left| \frac{Measr_i - Model_i}{Measr_i} \right| \right] \times 100 \quad (10)$$

$$NSE = 1 - \left[\frac{\sum_{i=1}^n (Measr_i - Model_i)^2}{\sum_{i=1}^n (Measr_i - \overline{Measr})^2} \right] \quad (11)$$

where $Measr$ is the measurement, $Model$ is the predictive equation and n is the total number of data.

3.0 RESULTS AND DISCUSSION

In order to understand the relationship between the wave overtopping and the governing parameters, wave height and water depth, results are plotted, and trends are discussed for mean overtopping discharge and maximum individual overtopping volume. Then, comparisons between the measured and predicted overtopping parameters based on the widely used empirical equation are presented. Finally, comparisons between the mean overtopping volume and the maximum individual overtopping volume are reported and discussed.

3.1 Mean Wave Overtopping Discharge

Figure 9 shows the relationship between mean wave overtopping discharge, q and wave height, H_{m0} for two water depths.

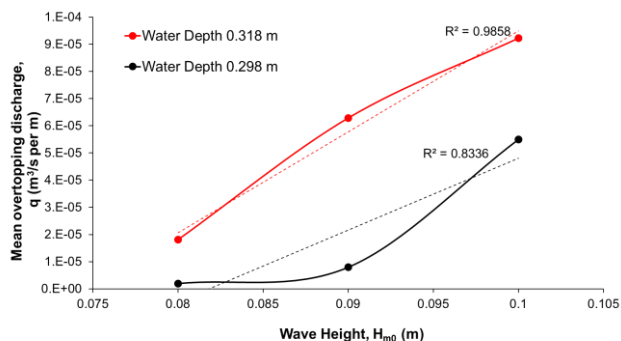


Figure 9 Mean overtopping discharge against wave height for two water depths, 0.318 m and 0.298 m

Overall, the mean overtopping discharge for water depth 0.318 m is higher than that for the water depth of 0.298 m. The wave overtopping discharge increases approximately 10 times for wave heights of 0.08 m and 0.09 m, and increases 1.7 times for the wave height of 0.1 m, when the water depth was raised to 0.318 m. The observed increase in mean overtopping discharge as the water depth was raised is attributed to the reduction of freeboard level, which allows more water to overtop the structure.

Figure 9 illustrates that as the wave height increases, so does the mean overtopping discharge. This shows that the mean overtopping discharge is influenced by the wave height. As the wave height increases, the wave energy would also increase, which would result in stronger waves and allow for more overtopping events to occur [25]. However, it can be observed that the influence of wave height on the mean overtopping discharge depends on the water depth. At the water depth of 0.298 m, wave heights smaller than 0.10 m were effectively dissipated on the slope, and, therefore, less overtopping discharge occurred.

Furthermore, as shown in Figure 9, R^2 values for both water depths 0.318 m and 0.298 m are 0.9858 and 0.8336, respectively. This shows that the variations of independent variable and dependent variable are larger for mean wave overtopping results of water depth 0.318 m than water depth 0.298 m.

The mean wave overtopping results are presented in Figure 10 with dimensionless parameters. The dimensionless parameters are used to provide direct comparison between various tests as proposed by Williams [26]. The freeboards tested are 0.073 m and 0.093 m for water depths 0.318 m, and 0.093 m, respectively.

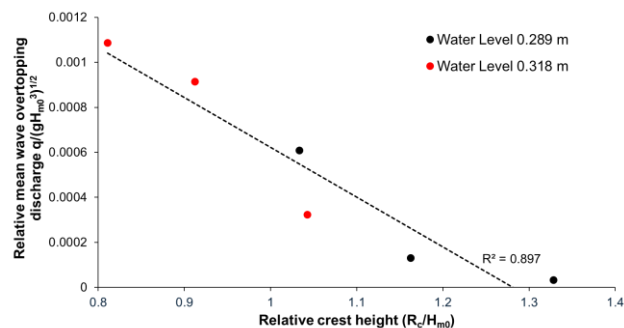


Figure 10 Relationship between relative mean wave overtopping discharge and relative crest height

Figure 10 shows that R_c/H_{m0} and $q/\sqrt{gH_{m0}^3}$ has an inversely proportional correlation. A large value of R_c/H_{m0} would reduce the relative overtopping discharge. The test scenarios with different freeboard levels, R_c demonstrate that the mean overtopping discharge is well represented by the formula similar to that proposed by Van der Meer [14]. The linear regression coefficient R^2 of 0.897 indicates a good fit data.

3.2 Maximum Individual Wave Overtopping

Each instance of wave overtopping was documented, enabling the identification of the maximum individual wave overtopping volume based on the highest recorded volume among the series of overtopping events. The largest value of individual wave overtopping is defined as V_{max} .

Figure 11 shows an example of large overtopping event captured during the experimental test. The overtopping phenomenon is described by the “Green water” wave overtopping from a non-breaking wave as described by Bruce et., al [24].



Figure 11 The occurrence of the large individual wave overtopping during the experiment

By referring to Figure 12, the V_{max} values increase as the wave height increases. Based on the time series of waves recorded in HR Merlin software, a higher wave height would allow higher maximum peak wave conditions, leading to larger overtopping volume.

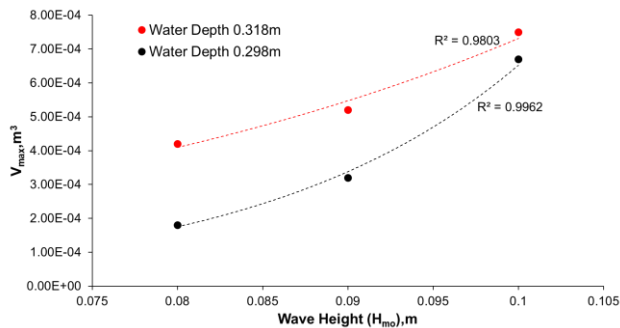


Figure. 12 Maximum individual wave overtopping volume V_{max} against wave height for water depths of 0.318 m and 0.298 m

From Figure 12, it is observed that water depth of 0.318 m gives higher V_{max} compared to lower water depth of 0.298 m. The V_{max} increased by 57% for the wave height of 0.08 m, 38% for the wave height of 0.09 m and 10% for wave height of 0.10 m, as the water depth raised to 0.318 m. The reduction of freeboard has led to the expected increase in V_{max} . Comparing these two results, it demonstrates that the percentage difference is higher for lower wave height, and the percentage difference gets smaller as the wave height increases. This trend may partly be explained by the fact that the freeboard significantly influences the energy dissipation for a lower wave height, and the influence decreases as the wave height increases. Furthermore, as shown in Figure 12, regression coefficient values for both water depths 0.318 m and 0.298 m are 0.9508 and 0.9423, respectively, indicating a good agreement between input variables and output variables.

Overall, the results suggest that both the mean overtopping discharge and the maximum individual wave overtopping volume are considerably affected by water depth and wave height variation, with similar trends observed for both overtopping parameters. A significant proportion of the incident wave energy is dissipated during the run-up on the slope. As the water depth increases, the structure slope area above the still water level, which is an important mechanism for wave energy dissipation, is now reduced. A lower proportion of energy dissipation should be expected within the smaller slope area; therefore, the overtopping volume will increase. Furthermore, the wave height is proportional to the wave energy. An increase in the wave height increases the wave energy and, consecutively, the overtopping.

3.3 Comparison between Measured and Predicted Wave Overtopping

Mean wave overtopping discharge: Figure 13 shows the comparison between measured mean

overtopping discharges and predicted mean overtopping discharges. The predicted mean overtopping was computed using Equation 1. The statistical analyses were conducted to further assess the performance and accuracy of the predictive model. Table 2 shows the three error indices, calculated for the mean wave overtopping volumes. The RMSE, MAPE, and NSE, are 7.61×10^{-6} m³/s/m, 12.8%, and 0.945 respectively. The low RMSE with the MAPE that is less than 20% indicate a good performance between the predictive equation and measurement. The NSE is greater than 0.9, inferring a nearly perfect model fit to the measured data. The results indicates that the measured mean overtopping discharges align consistently within the 80% confidence interval of the empirical values. This demonstration suggests that the empirical formula effectively represents the mean overtopping discharge.

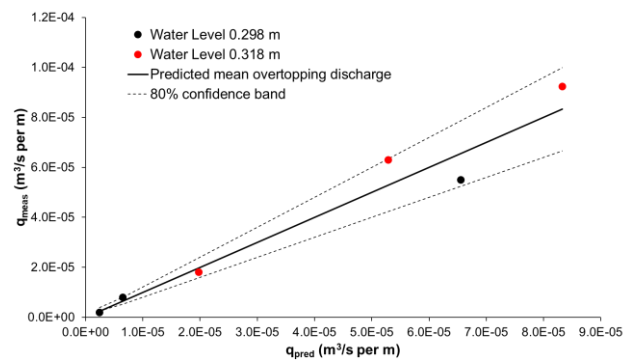


Figure 13 Comparison between measured and predicted mean wave overtopping discharge

Table 2 Statistical error index

Error Index	Mean wave overtopping volume, q_{mean}	Maximum individual wave overtopping volume, V_{max}
RMSE	7.61×10^{-6} m ³ /s/m	6.64×10^{-5} m ³
MAPE	12.8 %	17 %
NSE	0.945	0.912

Individual wave overtopping volume: Figure 14 demonstrates the comparison between predicted and observed maximum individual wave overtopping volume. The predicted maximum individual overtopping was computed using Equation 3. Results from the statistical analyses, as shown in Table 2, indicate a good performance of the predictive model. The RMSE, MAPE, and NSE, are 6.64×10^{-5} m³, 17%, and 0.912 respectively.

The measured maximum individual overtopping volumes lie within the confidence bound; however the first three values are slightly beyond the range. This may be due to the variation in shape factor, b of the distribution for individual wave overtopping volume. A study performed by Zanuttigh [23] on the shape factor, b obtained from the experimental

measurement shows that the factors were higher than the shape factor, b obtained from an empirical formula, for relatively low overtopping waves which then influenced the amount of maximum individual overtopping volume. Thus, it can be concluded that the shape factor used in the empirical formula is anticipated to offer more accurate predictions, especially in scenarios involving significant wave overtopping volumes.

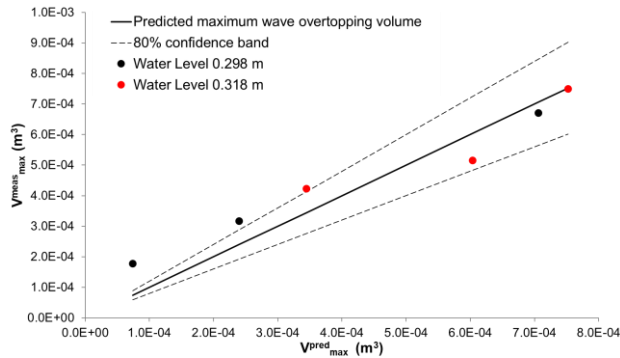


Figure 14 Comparison between measured and predicted maximum individual wave overtopping volume

Probability of overtopping: The study revealed that the variability of wave overtopping discharge correlated with the quantity of overtopping [26]. Therefore, as determined by the predictive analysis of numerical modelling by Williams [26], additional analysis was undertaken to ascertain whether the variations in discharge quantity are directly linked to the probability of wave overtopping, P_{ov} for a physical model test. P_{ov} is defined by N_{ow}/N_w where N_{ow} is the total number of overtopping waves and N_w represents the total number of waves generated in each test by the wave paddle. N_{ow} was evaluated for each overtopping event occurred while N_w was obtained from the zero-crossing statistics analysis in HR DAQ software. The prediction of probability of wave overtopping was obtained using empirical equation of Equation 5.

Figure 15 shows the relationship between the probability of wave overtopping and relative mean overtopping discharge as well as the comparison with the prediction probability of wave overtopping using the Van der Meer [14] equation. The higher probability of wave overtopping, the higher the relative mean wave overtopping discharge. Thus, it shows that the probability of wave overtopping, indeed influenced the variability of mean wave overtopping discharge.

From Figure 15, it shows that the Van der Meer [14] formula provides an underestimation of N_{ow} except for the largest overtopping discharge. This occurs due to the shallow water condition and the depth-limited wave condition ($H_{m0}/d > 0.2$), resulting in a more uniform distribution of individual wave overtopping volumes, with numerous occurrences of relatively large overtopping volumes [27]. Thus, fewer overtopping waves are needed to obtain the same

value of mean wave overtopping discharge as in deep-water condition.

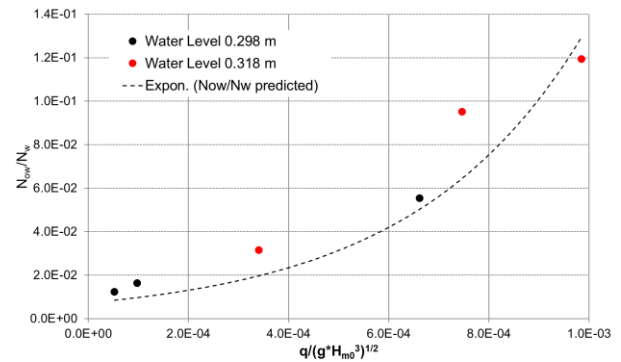


Figure 15 Evaluation of probability of wave overtopping against relative mean wave overtopping

In summary, the measured data was compared with the empirical equations presented in the EurOtop manual. The equations are widely adopted for engineering design and assessment purposes. It is essential to note that the equations are derived based on a large dataset comprising a wide range of structural and hydraulic parameters for broad practical engineering applications. Therefore, slight discrepancies between the measured data with a specific structural configuration and the predictions based on general equations should be acceptable. Discrepancies between the EurOtop empirical equations and the experimental results for tests on the rubble mound seawall by [11] and the breakwater by [18] were also reported. Nevertheless, the relationship between the governing parameters is well described and presented by the empirical equations.

Vmean versus Vmax: Figure 16 shows the comparison between the mean wave overtopping volume (V_{mean}) and maximum individual wave overtopping volume (V_{max}). It is clearly shown that the maximum individual wave overtopping is greater than the mean wave overtopping volume as depicted in bar charts of Figure 16. The percentage difference between both parameters is presented in Table 3.

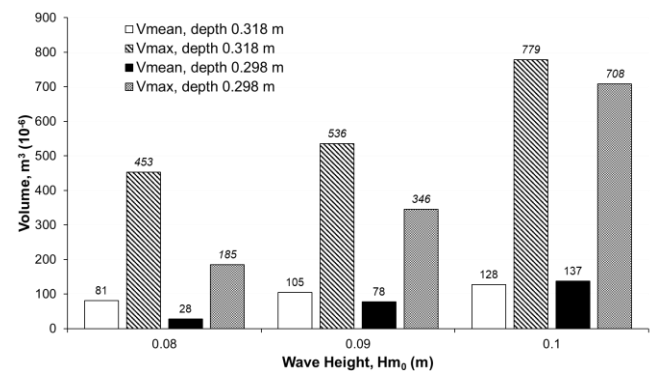


Figure 16 Comparison between maximum individual wave overtopping, V_{max} and mean wave overtopping volume, V_{mean} . Numbers on bars indicate the wave overtopping volume

Table 3 Percentage difference between mean wave overtopping volume and maximum individual wave overtopping volume

Wave Height, H_{mo} (m)	Water level, h , (m)	Mean wave overtopping volume, (m^3) [$\times 10^{-6}$]	Maximum individual wave overtopping volume, (m^3) [$\times 10^{-6}$]	Percentage difference* (%)
0.08	0.318	81	435	82
	0.298	28	185	85
0.09	0.298	105	536	80
	0.318	78	346	77
0.10	0.318	128	779	84
	0.318	137	708	81

*Percentage difference is determined using Eq. 8.

The percentage difference between V_{max} and V_{mean} is up to 85%, indicating that the influence of maximum individual wave overtopping volume is significant and should be considered as an alternative design parameter for coastal structures to avoid any possible hazard to humans and environment. Additionally, the variation in the volume of water that overtopped significantly differs from the mean wave overtopping volume. This discrepancy suggests that the mean wave overtopping volume may not fully capture the irregular and random nature of the overtopping phenomenon [28].

Under irregular wave conditions, the overtopping volume sharply varies from wave to wave. Low wave height typically gives a small overtopping volume, whereas large wave height may give a large overtopping volume. While the mean discharge represents the average discharge over the duration of the wave series, the maximum individual volume represents the highest volume resulting from the most severe wave in the wave series. Therefore, the maximum individual overtopping volume is expected to be considerably different than the mean overtopping discharge parameter. The maximum individual overtopping volume is a significant parameter that describes how severe wave overtopping can be.

In the design of coastal structures, the mean overtopping discharge parameter is often used to determine the crest level of the structure by ensuring the mean discharge associated with the crest level remains below the design criteria [29]. Based on the current practice, it is sufficient to use the mean discharge parameter for an optimized crest design [30]. On the other hand, the maximum individual overtopping volume may be of greater significance in some circumstances, such as when evaluating the potential damage to the structure due to wave overtopping and the safety of the public during an extreme event [31].

4.0 CONCLUSION

The wave overtopping responses including mean wave overtopping discharge and maximum individual wave overtopping volume have been analysed on rock

revetment structure through a physical model setup. Results from the experimental study were also compared with the prevalent empirical formula of EurOtop Manual [14]. The experimental tests performed in this study lead to several conclusions.

The wave height significantly influences the quantity of wave overtopping. The higher the wave height, the larger the wave overtopping. This indicates that higher waves would produce stronger waves, which lead to an increase in overtopping occurrences. The quantity of wave overtopping is also greater when the depth of water at the toe of the structure is increased because the freeboard level is lower, resulting in a greater discharge of wave overtopping. The amount of wave overtopping is directly related to the probability of wave overtopping ($N_{ow}N_w$). Larger wave overtopping discharges have a higher number of overtopping waves, N_w .

In addition, the variability of measured overtopping values falls within the specified reliability limits unless the conditions differ from the actual criteria of the equation used. Additionally, the maximum individual wave overtopping volume surpasses the mean wave overtopping volume by up to 85%, highlighting its importance as a wave overtopping parameter to be considered in designing coastal protection structures, thereby minimizing risks to both humans and infrastructure in the future. The possible hazards of extreme wave overtopping include death and injury to individuals located behind the coastal structure due to direct impact of waves. Additionally, there is a potential for damage to infrastructure and the failure of coastal structures, which could lead to coastal flooding.

Acknowledgments

The study was supported by Universiti Putra Malaysia research grant, vote number GP-IPS/2022/9709200 and authors' personal funds.

Conflicts of Interest

The author(s) declare(s) that there is no conflict of interest regarding the publication of this paper.

References

- [1] Tarakcioglu, G. O., Kisacik, D., Gruwez, V., & Troch, P. 2023. Wave Overtopping at Sea Dikes on Shallow Foreshores: A Review, an Evaluation, and Remaining Challenges. *Journal of Marine Science and Engineering*. 11(3).
- [2] Koosheh, A., Etemad-Shahidi, A., Cartwright, N., Tomlinson, R., & van Gent, M. R. A. 2021. Individual Wave Overtopping at Coastal Structures: A Critical Review and The Existing Challenges. *Applied Ocean Research*. 106: 102476.
- [3] Adibhusana, M. N., & Ryu, Y. 2024. Image-based Measurement Method of Overtopping Flow Velocity and Layer Thickness in Irregular Wave Conditions. *Journal of Coastal Research*. 116(sp1).

- [4] Schüttrumpf, H., & van Gent, M. R. A. 2004. Wave Overtopping at Seadikes. *Coastal Structures*. 431–443.
- [5] Shi-Igai, H. & Rong-Chung H. S. U. 1977. An Analytical and Computer Study on Wave Overtopping. *Coastal Engineering*. 1: 221–241.
- [6] Van der Meer, J. W. and Janssen, J. P. F. M. 1995. Wave Run-up and Wave Overtopping at Dikes. *Wave Forces on Inclined and Vertical Structures*. ASCE. 1: 1–27.
- [7] Van der Meer, J. W., Tönjes, P. and de Waal, J. P. 1998. A Code for Dike Height Design and Examination. *Proc. Conf. Coastlines, Structures and Breakwaters*, I.C.E. 5–19
- [8] Zhang, Y., Chen, G., Hu, J., Chen, X., Yang, W., Tao, A., & Zheng, J. 2017. Experimental Study on Mechanism of Seadike Failure due to Wave Overtopping. *Applied Ocean Research*. 68: 171–181.
- [9] Hassan, M. A., & Mohamad Ismail, M. A. 2018. Effect of Soil Types on the Development of Matric Suction and Volumetric Water Content for Dike Embankment during Overtopping Tests. *Civil Engineering Journal*. 4(3): 668–688.
- [10] van Gent, M. R. A. 2003. Wave Overtopping Events at Dikes. *Proceedings of the 28th International Conference on Coastal Engineering*. 2203–2215.
- [11] Koosheh, A., Etemad-Shahidi, A., Cartwright, N., Tomlinson, R., & van Gent, M. R. A. 2022. Distribution Of Individual Wave Overtopping Volumes at Rubble Mound Seawalls. *Coastal Engineering*. 177: 104173.
- [12] González, A. A., & Dopico, J. R. 2021. LPWAN in Civil Engineering. *Advances in Wireless Technologies and Telecommunication*. 223–244.
- [13] N. W. H. Allsop, T. Pullen, T. Bruce, J. W. Van der Meer, H. Schüttrumpf and A. Kortenhaus. 2007. *EurOtop 2007 Wave Overtopping of Sea Defences and Related Structures–Assessment Manual*. Boyens Medien GmbH & Co.
- [14] Van der Meer, J. W., Allsop, N. W. H., Bruce, T., De Rouck, J., Kortenhaus, A., Pullen, T., Schüttrumpf, H., Troch, P., Zanuttigh, B., Rouck, J. De, Kortenhaus, A., Pullen, T., Schüttrumpf, H., Troch, P., & Zanuttigh, B. 2016. Manual on Wave Overtopping of Sea Defences and Related Structures. An Overtopping Manual Largely based on European Research, but for Worldwide Application. *Report*. 264. www.overtopping-manual.com.
- [15] Yuhi, M., Mase, H., Kim, S., Umeda, S., & Altomare, C. 2021. Refinement of Integrated Formula of Wave Overtopping and Runup Modeling. *Ocean Engineering*. 220: 108350.
- [16] Christensen, N. F., Røge, M. S., Thomsen, J. B., Andersen, T. L., Burcharth, H. F., & Nørgaard, J. Q. H. 2014. Overtopping on Rubble Mound Breakwaters for Low Steepness Waves in Deep and Depth Limited Conditions. *Coastal Engineering Proceedings*. 1(34): 6.
- [17] van der Meer, J. W., Allsop, N. W. H., Bruce, T., de Rouck, J., Kortenhaus, A., Pullen, T., Schüttrumpf, H., Troch, P., Zanuttigh, B. 2018. *EurOtop 2018 Wave Overtopping of Sea Defences and Related Structures–Assessment Manual*. Boyens Medien GmbH & Co.
- [18] Bruce, T., van der Meer, J., Franco, L., & Pearson, J. M. 2007. A Comparison of Overtopping Performance of Different Rubble Mound Breakwater Armour. *Coastal Engineering*. 5: 4567–4579.
- [19] Strain, E. M. A., Kompas, T., Boxshall, A., Kelvin, J., Swearer, S., & Morris, R. L. 2022. Assessing the Coastal Protection Services of Natural Mangrove Forests and Artificial Rock Revetments. *Ecosystem Services*. 55: 101429.
- [20] Liew, M., & Xiao, M. 2020. Engineering Challenges and Options in Remediation and Prevention of Permafrost Coastal Erosion. *Geo-Congress 2020*. 881–889.
- [21] Sanitwong-Na-Ayuththaya, S., Saengsupavanich, C., Ariffin, E. H., Ratnayake, A. S., & Yun, L. S. 2023. Environmental Impacts of Shore Revetment. *Heliyon*. 9(9): e19646.
- [22] Christensen, N. F., Røge, M. S., Thomsen, J. B., Andersen, T. L., Burcharth, H. F., & Nørgaard, J. Q. H. 2014. Overtopping on Rubble Mound Breakwaters for Low Steepness Waves in Deep and Depth Limited Conditions. *Coastal Engineering Proceedings*. 1(34): 6.
- [23] Zanuttigh, B., Van der Meer, J. W., Bruce, T., & Hughes, S. A. 2013. Statistical Characterisation of Extreme Overtopping Wave Volumes The Procedure for Data Elaboration at Low-Crested Breakwaters. *Proc. Coasts, Marine Structures and Breakwaters*. 1: 442–452.
- [24] Bruce, Tom & Muller, Gerald & Allsop, William & Kortenhaus, Andreas. 2009. Criteria for Wave Impacts at Coastal Structures. *Coastal Structures*. 853–864. 10.1142/9789814282024_0075.
- [25] Xie, D., Zou, Q.-P., Mignone, A., & MacRae, J. D. 2019. Coastal Flooding from Wave Overtopping and Sea Level Rise Adaptation in the Northeastern USA. *Coastal Engineering*. 150: 39–58.
- [26] Williams, H. E., Briganti, R., Romano, A., & Dodd, N. 2019. Experimental Analysis of Wave Overtopping: A New Small Scale Laboratory Dataset for the Assessment of Uncertainty for Smooth Sloped and Vertical Coastal Structures. *Journal of Marine Science and Engineering*. 7(7): 217.
- [27] Nørgaard, J. Q. H., Lykke Andersen, T., & Burcharth, H. F. 2014. Distribution of Individual Wave Overtopping Volumes in Shallow Water Wave Conditions. *Coastal Engineering*. 83: 15–23.
- [28] Salauddin, M., & Pearson, J. M. 2018. Distribution of Wave by Wave Overtopping Volumes at Vertical Seawalls. *3rd International Conference on Protection against Overtopping*, 6-8 June 2018, UK.
- [29] CIRIA. 2007. The Rock Manual. *The Use of Rock in Hydraulic Engineering* (2nd Edition). In CIRIA, London.
- [30] Samion, M. K. H., Hamzah, S. B., & Desa, S. M. 2020. Stability and Overtopping Assessment of Tanjung Piai Stone Revetment via Two-Dimensional Hydraulic Modelling. In *Lecture Notes in Civil Engineering*. 53.
- [31] Raby, A., Jayaratne, R., Bredmose, H., & Bullock, G. 2020. Individual Violent Wave-overtopping Events: Behaviour and Estimation. *Journal of Hydraulic Research*. 58(1): 34–46.